

# Ultraviolet prepulse for enhanced x-ray emission and brightness from droplet-target laser plasmas

M. Berglund,<sup>a)</sup> L. Rymell, and H. M. Hertz

Department of Physics, Lund Institute of Technology, P. O. Box 118, S-221 00 Lund, Sweden

(Received 28 May 1996; accepted for publication 9 July 1996)

We show that an ultraviolet prepulse significantly enhances the water-window x-ray emission and brightness for a droplet-target laser plasma. By combining a 65 mJ, 120 ps,  $\lambda=532$  nm main pulse with an up to 3 mJ prepulse, the emitted x-ray photon flux may be increased more than eight times. The resulting C VI  $\lambda=3.37$  nm line emission is more than  $3 \times 10^{12}$  photons/sr·pulse, corresponding to a conversion efficiency above 3%/line. The integrated spectral brightness is increased two times and is found to reach its maximum for different prepulse parameters than those resulting in maximum photon flux. © 1996 American Institute of Physics. [S0003-6951(96)03938-1]

Laser-produced plasmas are attractive compact x-ray sources for, e.g., water-window microscopy and proximity lithography, due to their high brightness, small size, and high spatial stability.<sup>1</sup> Conversion efficiencies of several tens of percents have been achieved with conventional metal targets illuminated by laser intensities of  $\sim 10^{14}$  W/cm<sup>2</sup>.<sup>2</sup> However, the applicability of such solid-target laser plasmas are severely restricted due to the emission of debris, which may damage sensitive components positioned close to the plasma x-ray source. With liquid droplets as a target,<sup>3</sup> the debris problem is negligible<sup>4</sup> or eliminated.<sup>5</sup> By the use of ammonium hydroxide and fluorocarbon droplets, intense x-ray emission suitable for microscopy<sup>5</sup> and lithography,<sup>6</sup> respectively, is generated with a table-top arrangement. In this letter we show that an ultraviolet prepulse significantly enhances x-ray emission, conversion efficiency, and brightness of droplet-target line-emitting laser plasmas.

It is well known that the temporal characteristics of the laser pulse strongly influences the emitted x-ray photon flux from laser plasmas.<sup>7,8</sup> Previous prepulse experiments in the  $\sim 0.1$  ns pulse-width regime, which is the regime we normally use for water-window operation of the droplet-target x-ray source, show an enhancement in emitted keV x-ray flux by a factor 2–3.<sup>9,10</sup> In these references, the x-ray flux is found to increase monotonically with prepulse intensity before it saturates. The enhancement is explained by increased plasma volume,<sup>10</sup> in combination with increased inverse Bremsstrahlung absorption.<sup>9</sup> Prepulse studies has also attracted interest for subpicosecond pulses,<sup>11,12</sup> where such a pulse recently has been shown to be favorable for x-ray laser operation.<sup>13,14</sup> There are several methods for generating and applying the prepulse, e.g., splitting off a part of the beam,<sup>13,14</sup> using a  $\lambda=1.05$   $\mu\text{m}$  prepulse before the main  $\lambda=0.53$   $\mu\text{m}$  pulse with separate optics for the two beams<sup>9</sup> and extracting residual emitted laser radiation of the same wavelength but of different polarization than the main pulse.<sup>10</sup>

In this letter we describe a laser-energy-efficient method to generate an UV prepulse which, in combination with a visible main pulse, results in an enhancement in the emitted water-window x-ray photon flux by  $>8$  times. Equally im-

portant, we show that the source brightness can be increased  $\sim 2$  times and does not increase monotonically with prepulse energy. Instead, it reaches its maximum for different prepulse parameters than those which maximize the photon flux. In many imaging applications, e.g., microscopy,<sup>15</sup> the source brightness is more important than the total x-ray flux. Although very high water-window brightness may be produced with large-scale x-ray lasers,<sup>16</sup> compact systems still must rely on high-brightness incoherent sources. Finally, we discuss the influence of the prepulse on the x-ray pulse-to-pulse fluctuations.

The UV prepulse experimental arrangement is shown in Fig. 1. The droplet-target arrangement is briefly described below but for a more detailed presentation, see Refs. 3 and 17. Liquid ethanol at a pressure of  $\sim 40$  bars is injected into a  $10^{-4}$  mbar vacuum chamber through a  $\sim 10$   $\mu\text{m}$  capillary glass nozzle. Piezoelectric vibration of the nozzle creates a stable train of  $\sim 15$   $\mu\text{m}$  diam droplets at a rate of  $\sim 10^6$  drops/s. The 10 Hz active/active/passive mode-locked Nd:YAG laser (Continuum PY61C-10) is temporally synchronized with the piezoelectric vibration frequency in order to ensure that each laser pulse hits a single droplet.

The main pulse in this prepulse experiment is the  $\sim 65$  mJ,  $\sim 120$  ps,  $\lambda=0.53$   $\mu\text{m}$  frequency-doubled pulse which is extracted after the first second-harmonic generator (SHG) (cf. Fig. 1). After a variable delay, it is focused with an 80 mm best-form lens onto the droplets. The resulting  $\sim 12$   $\mu\text{m}$  FWHM focal spot corresponds to an intensity of

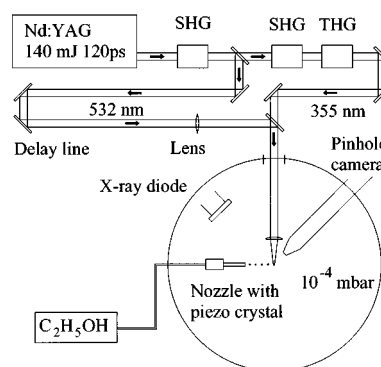


FIG. 1. Experimental arrangement for UV prepulse enhanced x-ray emission (SHG: second harmonic generator, THG: third harmonic generator).

<sup>a)</sup>Electronic mail: Magnus.Berglund@fysik.lth.se

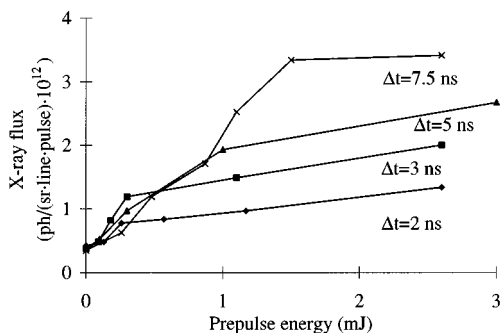


FIG. 2. X-ray emission in the  $\lambda=3.37$  nm C VI line as a function prepulse energy and temporal delay between prepulse and main pulse ( $\Delta t$ ).

$\sim 4 \times 10^{14}$  W/cm<sup>2</sup>. The prepulse utilizes the residual fundamental radiation ( $\lambda=1.06$   $\mu\text{m}$ ) after the extraction of the main pulse. This pulse is frequency tripled by two additional crystals, resulting in a few mJ/pulse at  $\lambda=0.35$   $\mu\text{m}$ . The UV wavelength of the prepulse allows efficient coupling of laser energy to the plasma.<sup>7</sup> The use of different wavelengths for the pre- and main pulses makes it easy to overlap the beams with wavelength-selective dielectric mirrors. Furthermore, by avoiding the fundamental IR laser wavelength, the risk of damages to the laser due to back-reflected light, e.g., from the plasma, is eliminated. After the variable delay of the  $\lambda=0.53$   $\mu\text{m}$  pulse, the two beams are brought to overlap spatially using a dielectric mirror on a fused silica substrate. Dispersion in the 80 mm focusing lens is compensated for with a long-focal-length lens (4 m) inserted in the  $\lambda=0.53$   $\mu\text{m}$  beam, allowing the two focuses to be accurately superimposed on the  $\sim 15$   $\mu\text{m}$  droplet.

In order to determine the prepulse dependence of the integrated spectral brightness (i.e., photons/sr·line· $\mu\text{m}^2$  pulse), both the x-ray photon flux (photons/sr·line·pulse) and the source area ( $\mu\text{m}^2$ ) must be determined. The water-window x-ray photon flux from the plasma was measured at a 45° angle to the incident laser beam with an x-ray diode (Hamamatsu G-1127-02) covered by a free-standing 160/100 nm Ag/Al sandwiched filter. With this filter the x-ray signal is dominated by the  $\lambda=3.37$ , 3.50, and 4.03 nm C VI and C V line emission.<sup>3</sup> The intensity ratio between these lines ( $\sim 3:1:3$ ) does not depend on prepulse condition, which was determined by spectral measurements using a 1 m grazing incidence monochromator (Minuteman 301-G). Thus, the photon flux from, e.g., the  $1s-2p$  C VI line at  $\lambda=3.37$  nm may be determined from the x-ray diode measurements with  $\pm 50\%$  accuracy.<sup>3</sup>

The source area was measured at 45° angle to the incident laser beam by a 55 $\times$  magnifying pinhole camera. By positioning an 8  $\mu\text{m}$  movable pinhole  $\sim 10$  mm from the source and recording the image with a 24 $\times$ 24  $\mu\text{m}$  pixel thinned back-illuminated x-ray sensitive CCD detector (Princeton Instruments), the FWHM diameter could be determined with better than 15% accuracy for plasmas larger than 9  $\mu\text{m}$  diameter. Emission at other wavelengths, including visible and ultraviolet stray light, was eliminated by the same Ag/Al filters as were used for the photon flux measurements.

Figure 2 shows the emitted photon flux in the  $\lambda=3.37$  nm C VI line as a function of prepulse energy for different

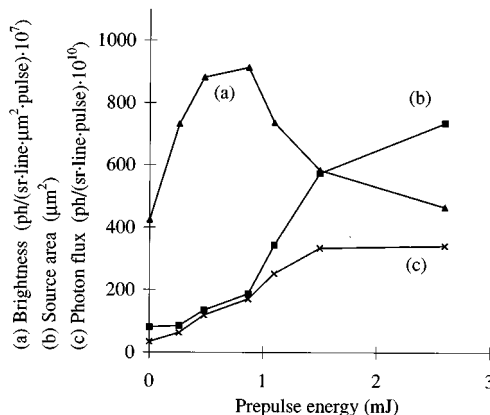


FIG. 3. Integrated spectral brightness, source area, and x-ray emission for  $\Delta t=7.5$  ns.

temporal delays between the prepulse and the main pulse ( $\Delta t$ ). The maximum emitted flux is  $> 3 \times 10^{12}$  photons/sr·line·pulse. Flux measurements in several directions indicate that emission is isotropic within  $\pm 25\%$ .<sup>4</sup> Thus, assuming uniform  $4\pi$  sr emission, the measured flux corresponds to a conversion efficiency of  $> 3\%$  per line and  $\sim 10\%$  for all carbon-ion lines in the water window. For larger prepulse energies and temporal delays than those indicated in Fig. 2, the x-ray flux saturates and decreases, respectively. Thus, for applications where only photon flux is an issue, the prepulse energy and the temporal delay must be matched to maximize the x-ray emission. Such an application is proximity lithography and contact microscopy, provided that the source size is sufficiently small to avoid penumbral blur.<sup>6</sup> Finally, it should be noted that we observe similar enhancement for the x-ray photon flux in other target liquids, e.g., ammonium hydroxide<sup>5</sup> and fluorocarbon,<sup>6</sup> emitting in the  $\lambda=1.2-3$  nm range.

In Fig. 3, the  $\lambda=3.37$  nm C VI line photon flux, source area (taken at half-maximum intensity) and integrated spectral brightness (photon flux/source area) are depicted for  $\Delta t=7.5$  ns. The brightness has a marked maximum for 0.5–0.8 mJ prepulse energy. This behavior is characteristic for all temporal delays investigated here. In many experiments the source should be optimized for brightness and not for photon flux. Such experiments include imaging x-ray microscopy or different forms of scanning x-ray microscopy (e.g., absorption or photoelectron), where the x-ray condenser or focusing optics, respectively, are used to produce a high-brightness focused spot.

Figure 2 shows that the x-ray flux enhancement is a function of both prepulse energy and delay time ( $\Delta t$ ). Basically, the prepulse creates an expanding plasma resulting in an increase in the inverse bremsstrahlung absorption of the subsequent  $\lambda=0.53$   $\mu\text{m}$  main pulse. However, the higher absorption alone cannot explain the  $> 8$  times flux enhancement since the absorption of single  $\lambda=0.53$   $\mu\text{m}$  pulses at  $\sim 4 \times 10^{14}$  W/cm<sup>2</sup> is  $\sim 60\%$ .<sup>7</sup> Furthermore, the larger enhancement recorded in the present measurements ( $> 8$  vs 2–3 in Ref. 9) suggests that factors in addition to plane-target volume enhancement<sup>9,10</sup> may contribute. Two such factors are (1) a higher volume enhancement, since the emit-

ting volume in the nearly spherically expanding droplet plasma grows faster than that of a linear-expansion plane-target plasma, and (2) the efficient deposition of the prepulse energy deep in the target due to the high critical electron density of the UV wavelength. For the longer  $\Delta t$ :s, the latter results in high absorption of the  $\lambda=0.53 \mu\text{m}$  pulse in a close to spherically expanding plasma with appropriate density for efficient recombination to the upper electronic levels and subsequent radiative line emission to the lower levels.<sup>18</sup> It is interesting to note that the combination of an UV main pulse with a  $\lambda=0.53 \mu\text{m}$  prepulse, results only in a negligible enhancement of the emitted x-ray flux.

For  $\Delta t=7.5 \text{ ns}$  in Fig. 2, the emitted x-flux saturates for high prepulse energies. At longer temporal delays the flux is lower for the same prepulse energies. The lower flux can be explained by the large plasma volume for large  $\Delta t$ :s. Since the target droplet has a limited mass, the average density of the large-volume plasma falls below the critical density regime suitable for high absorption. For the  $\Delta t=7.5 \text{ ns}$  case, a high prepulse energy is necessary to reach the saturation regime since a relatively large plasma volume of high density must be created. The decrease in the brightness in Fig. 3 starts slightly before the onset of the saturation regime when the projected area of the plasma volume grows faster than the photon flux. This decrease is more pronounced for longer  $\Delta t$ :s since the 3D expansion of the plasma volume around the droplet then has a larger impact on the projected emission area.

Our previous measurements of the water-window x-ray flux from the droplet target have typically been performed utilizing a small intrinsic prepulse resulting in  $\sim 1 \times 10^{12}$  photons/sr-line-pulse.<sup>3-5</sup> corresponding to an enhancement of  $\sim 3$  times. This pulse is emitted 7 ns before the main pulse by leaking part of the mode-locked pulse from the Nd:YAG laser cavity. Its average energy may vary but the intrinsic prepulse-to-prepulse variations are very large, resulting in shot-to-shot fluctuations of typically a factor 2–3 for a few mJ of average intrinsic prepulse energy. For similar prepulse energies, the UV prepulse described above reduces the fluctuations to  $\sim 25\%$  while still increasing the average x-ray flux nearly 3 times compared to the data for the intrinsic prepulse. For comparison, the flux fluctuations are  $<12\%$  when no prepulse is used. Reduction of pulse-to-pulse fluctuations facilitates single- or few-shot exposures in x-ray microscopy or lithography with correct exposure. The residual fluctuations in the x-ray flux are believed to be due to prepulse fluctuations ( $\sim 15\%$ ), main pulse fluctuations ( $\sim 7\%$ ), and small variations in droplet position with respect to the laser-beam focus.

In summary, we have enhanced the x-ray emission and

brightness from a table-top droplet-target laser plasma by  $>8$  and  $\sim 2$  times, respectively. The conversion efficiency is larger than 3%/line and for all lines into the water window it is  $\sim 10\%$ . This significantly improves table-top laser-plasma x-ray sources based on liquid droplet targets. In addition to the high flux and brightness, and negligible debris production discussed above, such sources allow long-term operation without interrupts, provide excellent geometric access, emit narrow-bandwidth radiation appropriate for zone-plate optics, allow spectrally tailored emission, and provide fresh target drops at high rates to match high-repetition-rate lasers. They are thus suitable compact sources for granular lithography, microscopy, or other x-ray applications.

The authors gratefully acknowledge Lars Malmqvist, the late Stig Borgström, and Charles Cerjan for valuable discussions, and Terje Rye, Siemens-Elementa AB, for donating capillary nozzles. This work was financed by the Swedish Research Council for Engineering Sciences, the Swedish Natural Science Research Council, and the Wallenberg Foundation.

- <sup>1</sup>See, e.g., F. Bijkerk, E. Louis, M. J. van der Wiel, E. C. I. Turcu, G. J. Tallents, and D. Batani, *J. X-Ray Sci. Technol.* **3**, 133 (1992); H. Daido, I. C. E. Turcu, I. N. Ross, J. G. Watson, M. Steyer, R. Kaur, M. S. Schulz, and M. Amit, *Appl. Phys. Lett.* **60**, 1155 (1992).
- <sup>2</sup>T. Mochizuki, T. Yabe, K. Okada, M. Hamada, N. Ikeda, S. Kiyokawa, and C. Yamanaka, *Phys. Rev.* **33**, 525 (1986).
- <sup>3</sup>L. Rymell and H. M. Hertz, *Opt. Commun.* **103**, 105 (1993).
- <sup>4</sup>L. Rymell and H. M. Hertz, *Rev. Sci. Instrum.* **66**, 4916 (1995).
- <sup>5</sup>L. Rymell, M. Berglund, and H. M. Hertz, *Appl. Phys. Lett.* **66**, 2625 (1995).
- <sup>6</sup>L. Malmqvist, L. Rymell, and H. M. Hertz, *Appl. Phys. Lett.* **68**, 2627 (1996).
- <sup>7</sup>C. Garban-Labaune, E. Fabre, C. E. Max, R. Fabbro, F. Amiranoff, J. Virmont, M. Winfeld, and A. Michard, *Phys. Rev. Lett.* **48**, 1018 (1982).
- <sup>8</sup>F. O'Neill, I. C. E. Turcu, D. Xenakis, and M. H. R. Hutchinson, *Appl. Phys. Lett.* **55**, 2603 (1989).
- <sup>9</sup>R. Kodama, T. Mochizuki, K. A. Tanaka, and C. Yamanaka, *Appl. Phys. Lett.* **50**, 720 (1987).
- <sup>10</sup>R. Weber and J. E. Balmer, *J. Appl. Phys.* **65**, 1880 (1989).
- <sup>11</sup>D. Kuehlke, U. Herpers, and D. von der Linde, *Appl. Phys. Lett.* **50**, 1785 (1987).
- <sup>12</sup>U. Teubner, G. Kuehnle, and F. P. Schäfer, *Appl. Phys. Lett.* **59**, 2672 (1991).
- <sup>13</sup>E. E. Fill, Y. Li, D. Schlögl, J. Steingruber, and J. Nilsen, *Opt. Lett.* **20**, 374 (1995).
- <sup>14</sup>J. Steingruber, S. Borgström, T. Starczewski, and U. Litzen, *J. Phys. B* **29**, L75 (1996).
- <sup>15</sup>J. Kirz, C. Jacobsson, and M. Howells, *Q. Rev. Biophys.* **28**, 33 (1995).
- <sup>16</sup>L. B. Da Silva, J. E. Trebes, R. Balthorn, S. Mrowka, E. Anderson, D. T. Attwood, T. W. Barbee, J. Brase, M. Corzett, J. Gray, J. A. Koch, C. Lee, D. Kern, R. A. London, B. J. MacGowan, D. L. Matthews, and G. Stone, *Science* **258**, 269 (1992).
- <sup>17</sup>H. M. Hertz, L. Rymell, M. Berglund, and L. Malmqvist, *Proc. SPIE* **2523**, 88 (1995).
- <sup>18</sup>E. J. Valeo and S. C. Cowley, *Phys. Rev. E* **47**, 1321 (1993).